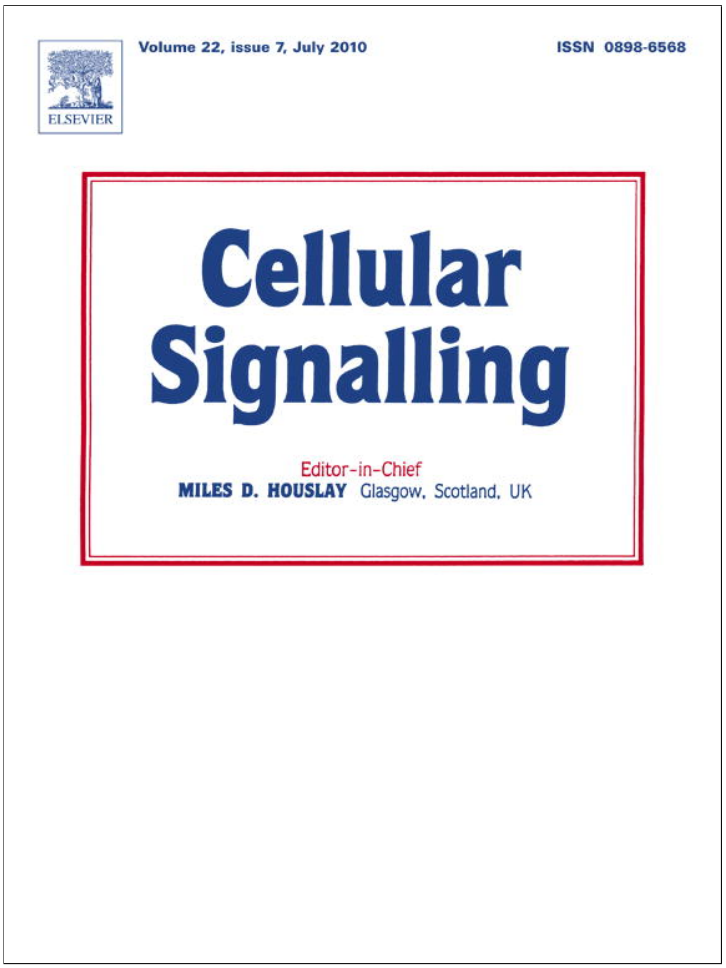

Cellular Signalling 22 (2010) 1044–1053

Contents lists available at ScienceDirect

Cellular Signalling

journal homepage: www.elsevier.com/locate/cellsig

Growth-dependent modulation of capacitative calcium entry in normal rat kidney fibroblasts

M.M. Dernison [a], W.H.M.A. Almirza [a], J.M.A.M. Kusters [b], W.P.M. van Meerwijk [a], C.C.A.M. Gielen [b], E.J.J. van Zoelen [a], A.P.R. Theuvenet [a,*]

[a] Department of Cell Biology, Radboud University Nijmegen, Heyendaalseweg 135, 6525 AJ Nijmegen, The Netherlands
[b] Department of Biophysics, Radboud University Nijmegen, Geert Grooteplein 21, 6525 EZ Nijmegen, The Netherlands

ARTICLE INFO

Article history:
Received 21 November 2009
Received in revised form 8 February 2010
Accepted 18 February 2010
Available online 24 February 2010

Keywords:
NRK fibroblasts
Store-operated calcium entry
Receptor-operated calcium entry
Growth stage
Calcium action potential

ABSTRACT

Normal rat kidney (NRK) fibroblasts have electrophysiological properties and intracellular calcium dynamics that are dependent upon their growth stage. In the present study we show that this differential behavior coincides with a differential calcium entry that can be either capacitative or non-capacitative. Confluent cells made quiescent by serum deprivation, which have a stable membrane potential near −70 mV and do not show spontaneous intracellular calcium oscillations, primarily exhibit the capacitative mechanism for calcium entry, also called store-operated calcium entry (SOCE). When the quiescent cells are grown to density-arrest in the presence of EGF as the sole polypeptide growth factor, these cells characteristically fire spontaneously repetitive calcium action potentials, which propagate throughout the whole monolayer and are accompanied by intracellular calcium transients. These density-arrested cells appear to exhibit in addition to SOCE also receptor-operated calcium entry (ROCE) as a mechanism for calcium entry. Furthermore we show that, in contrast to earlier studies, the employed SOCs and ROCs are permeable for both calcium and strontium ions. We examined the expression of the canonical transient receptor potential channels (Trpcs) that may be involved in SOCE and ROCE. We show that NRK fibroblasts express the genes encoding Trpc1, Trpc5 and Trpc6, and that the levels of their expression are dependent upon the growth stage of the cells. In addition we examined the growth stage dependent expression of the genes encoding Orai1 and Stim1, two proteins that have recently been shown to be involved in SOCE. Our results suggest that the differential expression of *Trpc5, Trpc6, Orai1 and Stim1* in quiescent and density-arrested NRK fibroblasts is responsible for the difference in regulation of calcium entry between these cells. Finally, we show that inhibition or potentiation of SOCE and ROCE by pharmacological agents has profound effects on calcium dynamics in NRK fibroblasts.

1. Introduction

There is currently a great interest in the cellular and molecular mechanisms that underlie store-operated calcium entry (SOCE). Upon release of intracellular calcium ions from stores in the endoplasmic reticulum (ER), calcium channels in the plasma membrane are opened, which results in an influx of calcium ions and a refilling of the intracellular stores. A breakthrough in the understanding of this process has come from the identification of the proteins Stim1 and Stim2 as sensors of Ca^{2+} within the ER. Stim proteins sense the depletion of Ca^{2+} from the ER, oligomerize, translocate to junctions adjacent to the plasma membrane, organize plasma membrane calcium channels into clusters and open these channels to bring about SOCE [1,2]. Recent studies have identified particular members of the Orai and Trpc family as the plasma membrane calcium channels that are activated by this calcium-store depletion mechanism [3].

Although the components that play a role in store-operated calcium entry may have been identified, relatively few studies have functionally characterized this process under physiological conditions. Calcium entry into cells can take place through voltage-dependent calcium channels, including L-type and N-type channels, or through voltage-independent calcium channels. The latter group can be subdivided into store-operated calcium channels (SOCs) and receptor-operated calcium channels (ROCs). SOCs are activated by depletion of calcium stores after calcium release, whereas ROCs are activated through PLC-coupled receptors involving second messengers such as diacylglycerol (DAG), inositol 1,4,5-trisphosphate (IP_3) and arachidonic acid (AA). Orai channels work according to a SOC mechanism, whereas certain members of the Trpc channel family operate as SOC, and others as ROC.

Abbreviations: SOCE, store-operated calcium entry; ROCE, receptor-operated calcium entry; NRK, normal rat kidney; $PGF_{2\alpha}$, prostaglandin $F_{2\alpha}$; OAG, 1-Oleoyl-2-acetyl-sn-glycerol; BHQ, 2,5-Di-t-butyl-1,4-benzohydroquinone; ER, endoplasmatic reticulum; 2-APB, 2-aminoethoxydiphenyl borate; IP_3, inositol 1,4,5-trisphosphate; Q-cells, quiescent NRK cells; DA-cells, density-arrested NRK cells.

* Corresponding author. Tel.: +31 243652013; fax: +31 243652999.
E-mail address: a.theuvenet@science.ru.nl (A.P.R. Theuvenet).

0898-6568/$ – see front matter © 2010 Elsevier Inc. All rights reserved.
doi:10.1016/j.cellsig.2010.02.007

In a number of studies we have made a detailed characterization of the calcium homeostasis in normal rat kidney (NRK) fibroblasts as a function of their growth status [4,5]. When cultured at high density in serum-free medium these cells become quiescent, which is characterized by a stable membrane potential near −70 mV. Addition of prostaglandin $F_{2\alpha}$ ($PGF_{2\alpha}$) to such quiescent cells, which activates the G-protein-coupled $PGF_{2\alpha}$-receptor (Ptgfr), results in degradation of inositol lipids and the production of IP_3, which releases calcium ions from the ER by activation of the IP_3-receptor. This process results in calcium oscillations, which are uncorrelated between different cells, and is accompanied by depolarization of the cells to a stable membrane potential of −20 mV. Upon addition of epidermal growth factor (EGF) and insulin to quiescent NRK cells, they can undergo one additional round of duplication, after which they stop proliferating as a result of density-dependent growth arrest. These density-arrested cells maintain a membrane potential near −70 mV, but show in addition periodically propagating calcium action potentials during which cells temporarily depolarize to positive values as a result of the opening of L-type calcium channels.

In an integrated model of calcium fluxes in NRK cells, we have previously shown that constitutive activation of plasma membrane calcium channels is essential for long-term calcium oscillations in $PGF_{2\alpha}$-treated quiescent cells, as well as for periodic calcium action potentials in density-arrested cells [6]. In the present study we have characterized experimentally the contribution of store-operated and receptor-operated calcium channels in the calcium homeostasis of quiescent and density-arrested NRK cells. Our results show that changes in calcium dynamics upon growing quiescent NRK cells to density-arrest coincide particularly with regulation of expression and activity of Trpc5, Trpc6 and Orai1 calcium channels, as well as of the calcium sensor Stim1.

2. Materials and methods

2.1. Cell culturing

Normal rat kidney fibroblasts (NRK clone 49F) were seeded at a density of 1.25×10^4 cells/cm^2 in bicarbonate-buffered Dulbecco's modified Eagle's medium (DMEM; Invitrogen, Carlsbad, CA) supplemented with 10% newborn calf serum (HyClone Laboratories, Logan, UT). Confluency was reached after four days. Cells were then incubated for three days in serum-free DF medium (1:1 mixture of DMEM and Ham's F-12 medium (Invitrogen)) supplemented with 30 nM Na_2SeO_3 and 10 μg/ml human transferrin, to obtain quiescent cells. Density-arrested monolayers were obtained by incubation of quiescent cells for 48 h with 5 ng/ml EGF (Collaborative Research Incorporated, Bedford, MA) in combination with 5 μg/ml insulin (Sigma-Aldrich, St. Louis, MO). For calcium imaging experiments 1.2×10^5 NRK cells were seeded on 0.1% gelatin-coated glass coverslips with a diameter of 25 mm in 9.6 cm^2 wells.

2.2. Intracellular calcium measurements

Glass coverslips grown with quiescent monolayers of NRK fibroblasts were placed in a cell chamber and loaded for 30 min with 4 μM Fura-2/AM (Molecular Probes, Eugene, OR) in serum-free DF medium at room temperature. Medium was replaced by Ca^{2+}-free HEPES-buffered saline (Ca^{2+}-free HBS, containing 143 mM NaCl, 5 mM KCl, 1 mM $MgCl_2$, 10 mM glucose, 10 mM HEPES-KOH, and pH 7.4). Ca^{2+} or Sr^{2+}-containing HBS (128 mM NaCl, 10 mM $CaCl_2$ or $SrCl_2$, 5 mM KCl, 1 mM $MgCl_2$, 10 mM glucose, 10 mM HEPES-KOH, and pH 7.4) was mixed with an equal amount of Ca^{2+}-free medium to obtain a 5 mM Ca^{2+} or Sr^{2+}-containing medium in the chamber. Dynamic calcium video imaging was performed as described elsewhere [7]. Excitation wavelengths of 340 nm and 380 nm (bandwidth 8–15 nm) were provided by a 150 W Xenon lamp (Ushio UXL S150 MO, Ushio, Tokio, Japan), while fluorescence emission was monitored above 440 nm, using a 440 nm DCLP dichroic mirror and a 510 nm emission filter (40 nm bandwidth) in front of the camera. Image acquisition, using a camera pixel binning of 4 and computation of ratio images (F340/F380), was every 4 sec and operated through Metafluor v.6.2 (Universal Imaging Corporation, Downingtown, PA). Camera acquisition time was 100 ms per excitation wavelength. The agents U73122, SKF96365, Gö6976 and OAG were purchased from Sigma-Aldrich (St. Louis, MO), BHQ was purchased from Calbiochem (Darmstadt, Germany) and 2-APB from Tocris (Avonmouth, UK).

2.3. Data analysis

At each measurement variations in intracellular calcium concentration as a function of time were measured simultaneously in 50 to 70 cells. The Mann–Whitney *U* ranking test was applied for comparing the frequency of calcium oscillations/transients in different cell groups. The increase of the F340/F380 ratio due to calcium influx through membrane channels or by calcium release from intracellular stores was determined by subtracting the mean ratio before (basal level) and after (peak) the calcium influx or release. Numerical data are represented as mean ± S.E.M throughout this article, with *n* representing the number of replicates in each experiment. Significance levels (denoted *p*) have been determined by double-sided student's *T*-test unless otherwise stated.

2.4. PCR primers and total RNA isolation

PCR primers for rat *Trpc1-7, Orai1* and *Stim1* were designed based on published sequences in GenBank (see Supplementary Table S1) using Oligo Perfect designed tool (Invitrogen). Total RNA was isolated from NRK cells using Trizol (Invitrogen) according to manufacturer's protocol.

2.5. RT-PCR

First strand cDNA was prepared from 1 μg of total RNA using SuperScript™ II RNase H^- reverse transcriptase (Invitrogen) and 0.25 μg of hexamer primer. Thereto RNA samples were denaturated at 65 °C for 55 min and reverse transcription was performed for 50 min at 42 °C and stopped by heating the samples for 15 min at 70 °C. The cDNA was amplified by PCR using the specific primers for individual *Trpc* genes (see list in Supplementary Table S1) and Taq polymerase™ (Invitrogen). PCR amplification was performed using a PERKIN ELMER Gene Amp PCR System 2400 (Norwalk, CT) using 1 μl of first stranded cDNA reaction, 150 pmol of each degenerate primer, 50 μM of dNTPs, 2 units of Taq polymerase and 2.5 mM $MgCl_2$ in total volume of 50 μl. PCR conditions were as follows: 3 min at 94 °C, 40 cycles consisting of 30 s at 94 °C, followed by 1 min at 72 °C. After completion of the 30 cycles, samples were incubated at for 10 min 72 °C. The PCR products were visualized on an ethidium bromide-stained agarose gel.

2.6. Quantitative real-time RT-PCR

The mRNA levels for genes of interest were analyzed by using quantitative RT-PCR (Detection System 5700 ABI Prism, Applied Biosystems, Foster City, CA). A total of 1 μg of cDNA, synthesized as described above using the primers shown in supplementary Table S2, was amplified using SYBR Green PCR Mastermix (Applied Biosystems) under the following conditions: initial denaturation for 10 min at 95 °C, followed by 40 cycles consisting of 15 s at 94 °C and 1 min at 60 °C. Expression values were calculated from threshold cycles at which an increase in reporter fluorescence above baseline signal could first be detected.

3. Results

3.1. Characterization of store-operated calcium entry in quiescent and density-arrested NRK fibroblasts

Store-operated calcium entry (SOCE) was studied in quiescent (Q) and density-arrested (DA) NRK fibroblasts by measuring calcium influx after release of calcium from intracellular stores. Emptying of these stores was induced by placing the cells in a nominal calcium-free medium in the additional presence of the sarco-endoplasmatic reticulum Ca^{2+}-ATPase (SERCA) inhibitor BHQ. SOCE was subsequently measured by increasing the extracellular calcium concentration to 5 mM.

Fig. 1 shows on the basis of the F340/F380 ratio of Fura-2 fluorescence that the release of calcium from the stores results in an increase in cytoplasmic calcium ions, which are rapidly pumped out of the cells by the plasma membrane Ca^{2+}-ATPase. Subsequent addition of calcium to the extracellular medium results in a strong, transient increase in cytoplasmic calcium concentration due to the activity of store-operated calcium channels. Fig. 1A shows that the release of calcium from intracellular stores in Q-cells resulted in an increase in F340/F380 ratio of 0.080 ± 0.008 (mean $\pm$ SEM, $n = 19$), as measured from the basal level to the peak value after the addition of BHQ. Addition of extracellular calcium ions resulted in a rise of the F340/F380 ratio of 0.14 ± 0.01 (mean $\pm$ SEM, $n = 19$), as measured from the basal level to the peak value after addition of Ca^{2+}. Comparable experiments for DA-cells (see Fig. 1B) resulted in an increase in F340/F380 ratio of 0.10 ± 0.02 (mean $\pm$ SEM, $n = 6$) for BHQ treatment and of 0.19 ± 0.02 (mean $\pm$ SEM, $n = 6$) upon subsequent calcium addition. Fig. 1C shows that addition of extracellular calcium to Q-cells without prior depletion of calcium stores by BHQ treatment resulted in a small increase in the F340/F380 ratio of only 0.030 ± 0.021 (mean $\pm$ SEM, $n = 4$). These data show that SOCE in density-arrested NRK cells is higher than in quiescent cells, although the difference was below the 95% confidence interval for statistical significance ($p = 0.08$).

Since DA-cells can undergo spontaneous calcium action potentials, accompanied by calcium influx due to transient opening of the L-type calcium channel, the above experiments were carried out in the presence of the L-type channel inhibitor nifedipine. Control experiments showed that nifedipine had no effect on the intracellular calcium level of both Q- and DA-cells (data not shown).

3.2. Characterization of receptor-operated calcium entry in quiescent and density-arrested NRK fibroblasts

Receptor-operated calcium entry (ROCE) was studied in quiescent (Q) and density-arrested (DA) NRK fibroblasts by pre-incubating the cells in nominal calcium-free medium with the DAG-analogue OAG and measuring the increase in intracellular calcium concentration upon addition of 5 mM extracellular Ca^{2+}. Nifedipine was added in the experiments to prevent calcium influx through voltage-dependent L-type calcium channels.

Fig. 2A shows that addition of extracellular calcium to Q-cells in the presence of OAG resulted in a F340/F380 increase of 0.045 ± 0.013 (mean $\pm$ SEM, $n = 10$) above the basal fluorescence level. Fig. 2B shows that the addition of calcium ions to OAG-treated DA-cells resulted in an increase in F340/F380 of 0.11 ± 0.01 (mean $\pm$ SEM, $n = 10$), which is 2.4 times higher ($p < 0.01$) than the value observed in Q-cells. When these experiments were carried out in DA-cells without prior incubation with OAG (Fig. 2C), a value of 0.11 ± 0.01 (mean $\pm$ SEM, $n = 10$) was found, which is not significantly different from the increase found in the presence of OAG. This suggests that density-arrested NRK cells may already contain sufficient DAG to activate receptor-operated calcium channels. Fig. 2D shows that pretreatment of DA-cells with PLC-inhibitor U73122 in order to prevent PIP_2 degradation and concomitant DAG production, reduced the increase in F340/F380 to 0.061 ± 0.007 (mean $\pm$ SEM, $n = 7$), which is indeed

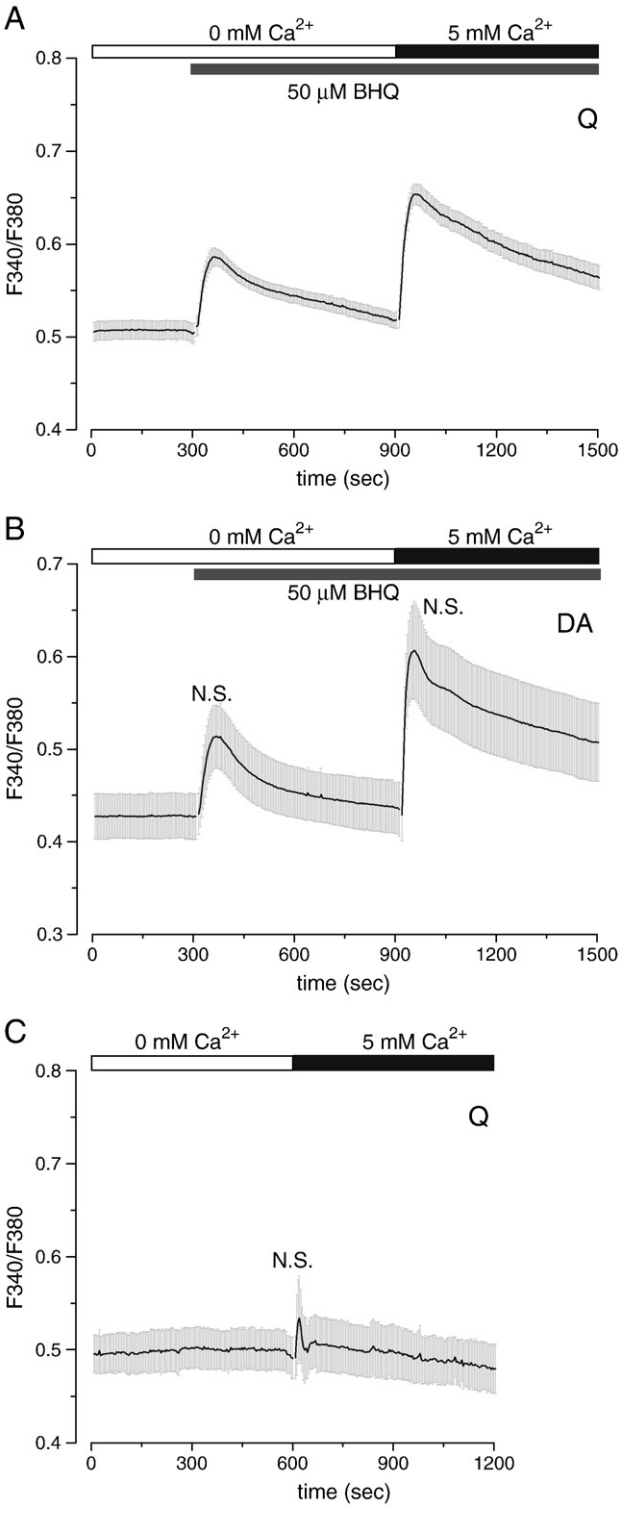

Fig. 1. Demonstration of store-operated calcium entry in NRK fibroblasts. Store-operated calcium entry is present in both quiescent (A) and density-arrested (B) NRK fibroblasts. BHQ (50 µM) was added to deplete intracellular calcium stores (first phase of calcium increase) and subsequently 5 mM extracellular calcium was added to induce store-operated calcium entry (second phase). Recordings in density-arrested cells were performed in the presence of nifedipine to prevent activation of L-type channels. Difference in the calcium entry between quiescent and density-arrested fibroblasts was not significant (N.S.). Addition of extracellular calcium to quiescent cells without previous stimulation did not induce a significant increase (N.S.) in the intracellular calcium level (C). The gray band around the traces represents the SEM-error bars for every datapoint.

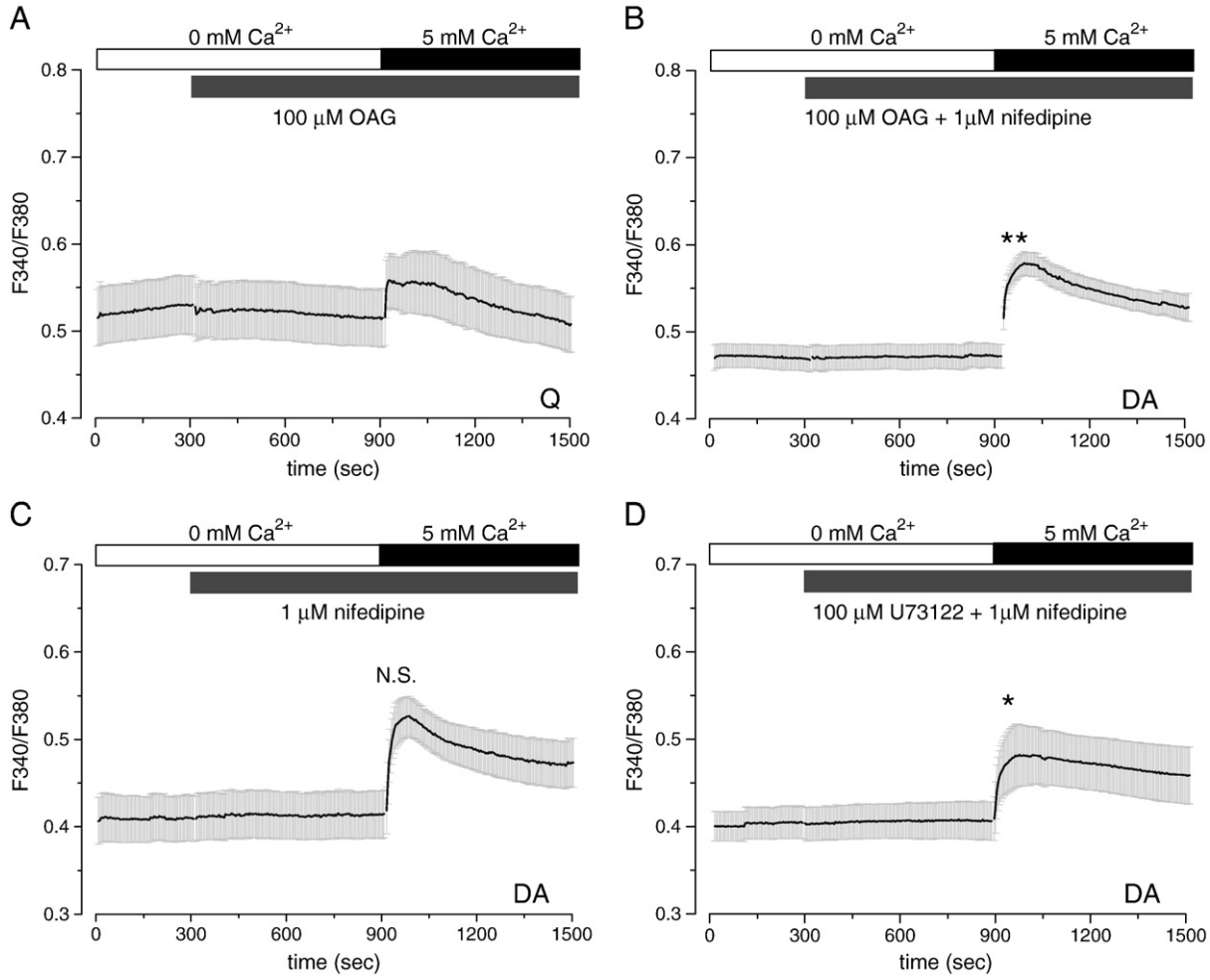

Fig. 2. Non-store-operated calcium entry is larger in density-arrested than in quiescent cells. Increase in intracellular calcium upon re-addition of calcium in the presence of 100 µM OAG to quiescent cells (A) and density-arrested cells (B) (significance: **, $p<0.001$, compared to A, $n=10$). Increase in intracellular calcium upon re-addition of calcium to density-arrested cells in the absence of OAG (N.S., compared to B, $n=10$) (C). Calcium entry upon re-addition of calcium to density-arrested cells in the presence of the PLC-inhibitor U73122 (D) (significance: *, $p<0.05$, compared to C, $n=7$). All recordings in density-arrested cells were performed in the presence of nifedipine to prevent entry of calcium through L-type calcium channels. The gray band around the traces represents the SEM-error bars for every datapoint.

45% lower than the value observed for these cells in the absence of this inhibitor, either with or without additional OAG.

These results show that density-arrested NRK cells display significantly higher levels of ROCE than quiescent cells. Furthermore they suggest that at least in density-arrested cells activation of receptor-operated calcium entry takes place in a PLC-dependent manner.

3.3. Mechanism of strontium uptake in NRK cells

We have previously shown that $PGF_{2\alpha}$-mediated calcium oscillations in quiescent, as well as spontaneous calcium action potentials in density-arrested NRK cells, also occur in the presence of externally added strontium ions [8]. These studies provided evidence that during an action potential L-type calcium channels can mediate the uptake of strontium ions into NRK cells. However, the ion channels involved in strontium uptake in the absence of an action potential have not been characterized yet. Fig. 3A, B compares the uptake of calcium and strontium ions, respectively, by store-operated ion channels in DA-cells. In BHQ-treated cells 5 mM Ca^{2+} induced a F340/F380 increase of 0.14 ± 0.01 (mean ± SEM, $n=19$), while 5 mM Sr^{2+} induced a fluorescence increase of 0.034 ± 0.008 (mean ± SEM, $n=11$). Fig. 3C, D shows the rise in fluorescence ratio by the uptake of calcium or strontium ions, respectively, through receptor-operated channels in OAG-treated DA-cells. Addition of calcium ions resulted in a F340/F380 increase of 0.11 ± 0.01 (mean ± SEM, $n=12$), while strontium ions induce an increase in fluorescence ratio of 0.075 ± 0.019 (mean ± SEM, $n=6$). These data indicate that strontium ions can be taken up by NRK cells through both store-operated and receptor-operated ion channels. All the measured increases of the fluorescence ratio in these experiments were significant compared to the baseline values.

When interpreting these data it should be taken into account that calcium and strontium ions both change the fluorescence properties of Fura-2, but do so with a different affinity (Ca^{2+}:$K_d=224$ nM; Sr^{2+}:$K_d=9.2$ µM [9]). The relatively small change in fluorescence upon addition of strontium ions therefore corresponds to a relatively high permeability of the plasma membrane for Sr^{2+}, when compared to calcium ions. Calibration of the Fura-2 ratio signal by the method of Grynkewic [10] was not conclusive due to the small increase in the fluorescence ratio when strontium was added. Based on the above K_d-values and the known Hill coefficient of Fura-2, the observed increase in fluorescence ratio from 0.52 to 0.65 after the addition of extracellular calcium (Fig. 3A) corresponds to an increase in intracellular calcium concentration of 0.44 µM. In comparison, the relatively small increase from 0.49 to 0.52 upon the addition of extracellular strontium (Fig. 3B) corresponds to an intracellular strontium concentration up to 10 µM. This indicates that strontium ions can permeate through store-operated ion channels at least as good as calcium ions. Moreover, the relatively high fluorescence increase for strontium versus calcium ions during receptor-operated ion uptake indicates that strontium ions are well taken up by NRK cells by both SOCE and ROCE mechanisms.

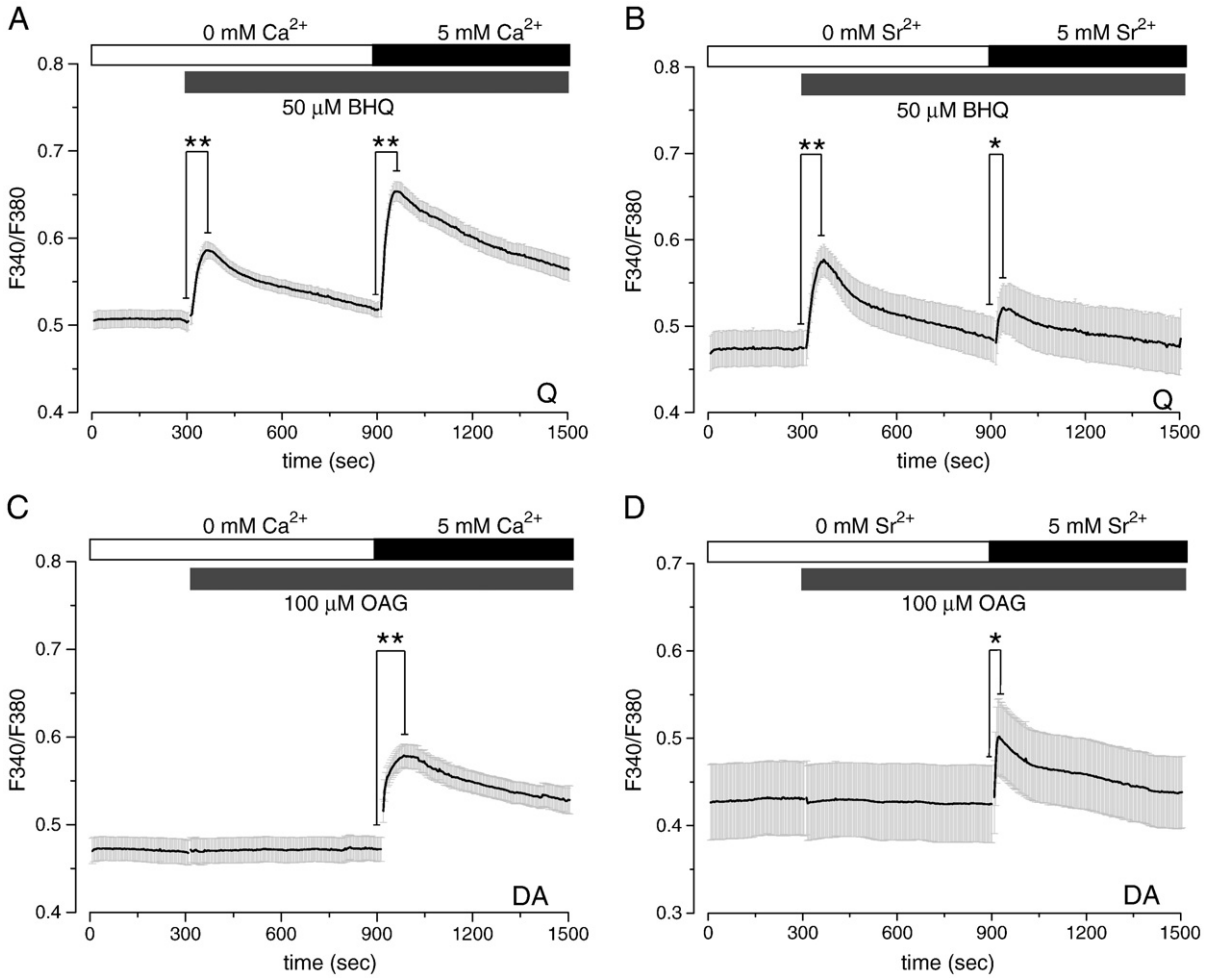

Fig. 3. ROCE and SOCE are permeable for calcium as well as strontium ions. Calcium (A) and strontium (B) entry after depletion of calcium stores induced by BHQ (50 μM) in quiescent cells. Receptor-operated calcium (C) and strontium (D) entry in density-arrested cells in the presence of OAG (100 nM) and nifedipine (1 μM). All changes in the F340/F380 fluorescence ratio where significant (peak values compared to the baseline) (significance: *, $p<0.002$; **, $p<10^{-6}$). The gray band around the traces represents the SEM-error bars for every datapoint.

3.4. Endogenous expression of Trpc family members, Orai1 and Stim1 in NRK fibroblasts

In order to test which calcium channels may be involved in the observed SOCE and ROCE, we tested NRK cells for expression of channel encoding genes by RT-PCR analysis. Fig. 4A shows that of the various Trpc channels, NRK cells expressed particularly the genes encoding Trpc1, Trpc5 and Trpc6. As a comparison, rat brain tissue expressed at least the genes encoding Trpc1, Trpc3, Trpc4, Trpc5, and Trpc6, but possibly also those encoding Trpc2 and Trpc7. Trpc1 is generally considered as a channel involved in SOCE [11], while Trpc6 is known to be DAG dependent [12]. Trpc5 is less well characterized in this respect. The observation that NRK cells express these three genes, confirms our functional studies that NRK cells contain both SOCs and ROCs. As shown in Fig. 4B, quantitative RT-PCR analysis indicated that particularly *Trpc5* (10-fold) and *Trpc6* (6-fold) are strongly up-regulated when quiescent NRK cells are grown to density-arrest. In contrast, the high expression level of *Trpc1* is not enhanced upon density-arrest of the cells.

Under similar experimental conditions, transcripts of both Stim1 and Orai1 were detected in NRK fibroblasts by RT-PCR. Fig. 5A, C shows the PCR products obtained for Stim1 and Orai1, respectively. Gel electrophoresis confirmed that the PCR product sizes corresponded to rat Stim1 (293 bp) and rat Orai1 (375 bp). Sequencing of the PCR products showed agreement with the original GenBank sequences. Upon density-arrest, the expression of *Stim1* and *Orai1* was up-regulated 1.6 and 5.5 fold, respectively (Fig. 5B, D).

Although these data do not necessarily reflect changes in channel densities, the results indicate that the genes for most calcium channels tested and for the calcium sensor Stim1 are strongly up-regulated, when NRK cells are grown from quiescence to density-arrest. These data agree with our functional studies showing that both SOCE and ROCE are clearly enhanced upon growing NRK cells to density-arrest (see Sections 3.1 and 3.2).

3.5. Calcium influx limits calcium oscillations

We have previously shown that calcium influx is required for the persistent calcium oscillations that are induced by $PGF_{2\alpha}$ in quiescent NRK cells [5]. Several pharmaceutical agents are known to inhibit or enhance SOCE and ROCE. We have determined the inhibitory or enhancing effect of three of these compounds. In Fig. 6 we show that 2-APB and SKF96365 had profound inhibitory effects on SOCE in quiescent (Fig. 6A, C, respectively) and ROCE in density-arrested cells (Fig. 6B, D, respectively) (see also Supplementary Table S3). In the remainder of Fig. 6 we show that pre-incubation with the protein kinase C inhibitor Gö6976 potentiated SOCE in quiescent cells (Fig. 6E) and also ROCE in density-arrested cells (Fig. 6F) (see also Supplementary Table S3). The present observations show that calcium entry into NRK cells can be either inhibited or enhanced by pharmacological treatments. Because of the inhibitory effects of 2-APB on IP_3 receptors [13], we choose SKF96365 and Gö6976 to test their inhibitory and potentiating effects, respectively, on $PGF_{2\alpha}$-induced

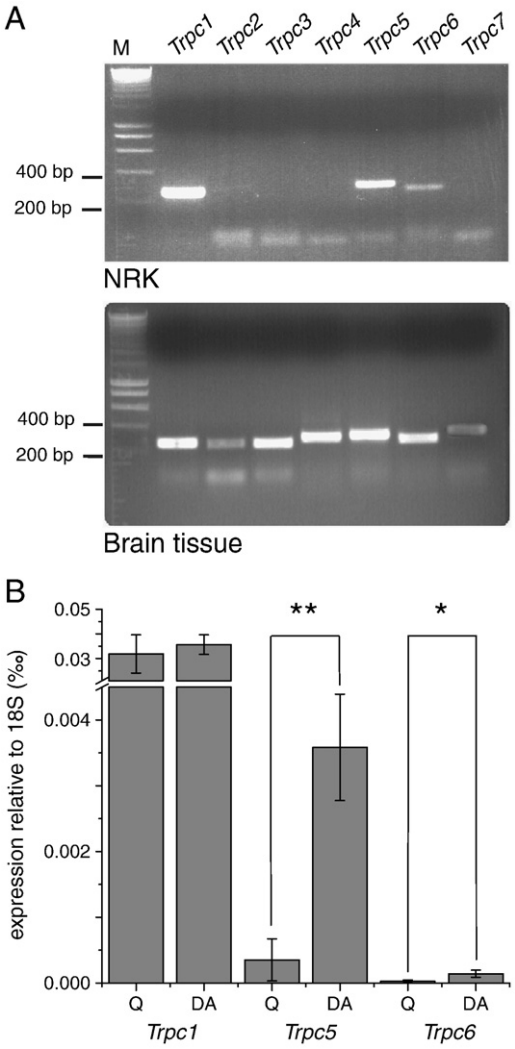

Fig. 4. Differential expression of *Trpc1*, *Trpc5* and *Trpc6* genes in quiescent and density-arrested NRK fibroblasts. (A) RT-PCR analysis of the expression of *Trpc* genes in NRK fibroblasts. Equal amounts of cDNA, prepared from quiescent NRK cells and rat brain tissue as a positive control, were added in combination with specific primers for individual *Trpc* genes (see Supplementary Table S1). Data are representative of three independent experiments. M denotes marker for base-pair length. B) mRNA levels for Trpc1, Trpc5 and Trpc6 in quiescent (Q) and density-arrested (DA) NRK fibroblasts determined by quantitative RT-PCR using *Trpc* specific primers (see Supplementary Table S2), and expressed relative to 18S rRNA levels. (significance: *, $p<0.05$; **, $p<0.005$, $n=4$).

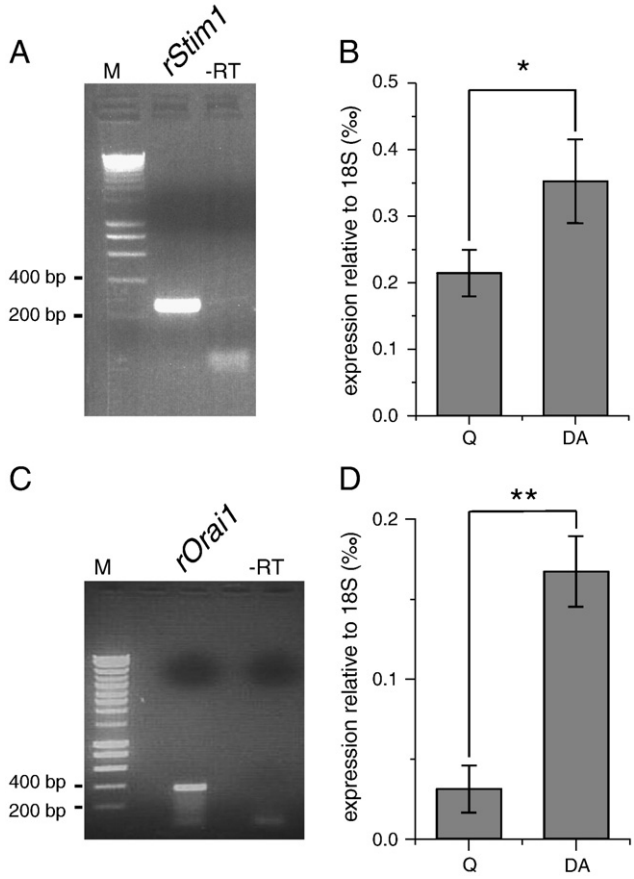

Fig. 5. Differential expression of Stim1 and Orai1 genes in quiescent and density-arrested NRK fibroblasts. RT-PCR analysis of Stim1 (A) and Orai1 (C) expression in NRK fibroblasts. Equal amounts of cDNA, prepared from quiescent NRK cells and rat brain tissue as a positive control, were added in combination with gene specific primers (see Supplementary Table S1). Data are representative of three independent experiments. mRNA levels of Stim1 (B) and Orai1 (D) in quiescent (Q) and density-arrested (DA) NRK fibroblasts determined by quantitative RT-PCR using gene specific primers (see Supplementary Table S2), and expressed relative to 18S rRNA levels (significance: *, $p<0.05$; **, $p<0.005$, $n=3$).

calcium oscillations and spontaneous action potential-induced calcium transients.

In Fig. 7 we show typical responses of individual quiescent cells upon inhibition and potentiation of SOCE. Fig. 7B shows that pre-incubation of Q-cells with Gö6976 resulted in an inhibition of $PGF_{2\alpha}$-induced calcium oscillations after approximately 10 min. In contrast, addition of SKF96365 resulted in an immediate decrease in the frequency of calcium oscillations (Fig. 7C). Density-arrested NRK cells display spontaneous action potentials with concomitant calcium transients. In Fig. 8 we show the typical responses of whole monolayers of density-arrested cells upon inhibition and potentiation of ROCE and SOCE. Fig. 8B shows that pre-incubation with Gö6976 had no significant effect on the frequency of the action potential-induced calcium transients in DA-cells. The addition of SKF96365 resulted in an immediate extinction of the spontaneous calcium spikes (Fig. 8C). Table 1 summarizes the results of the Mann–Whitney analysis of the effects of SKF96365 and Gö6976 on the $PGF_{2\alpha}$-induced calcium oscillations and the spontaneous calcium spikes, as exemplified in the Figs. 7, 8, respectively. The analysis revealed that in Q-cells potentiation by Gö6976 as well as inhibition by SKF96365 of calcium entry both significantly reduced the frequency of the $PGF_{2\alpha}$-induced calcium oscillations, while in DA-cells only inhibition of calcium entry caused a significant reduction in the frequency of the action potential-induced calcium transients.

4. Discussion

In this study we show a differential role for SOCs and ROCs in the calcium dynamics of quiescent and density-arrested NRK fibroblasts. For the first time the occurrence of both types of calcium entry has been demonstrated experimentally in quiescent and density-arrested NRK cells. In an earlier study we already predicted the necessity of a calcium entry pathway, dependent on the filling state of the intracellular calcium stores, which could have a stabilizing role in intracellular IP_3-mediated calcium dynamics and cell membrane excitability [6]. Here we show experimentally that this calcium store-dependent calcium entry is differentially regulated via SOCs and ROCs in quiescent and density-arrested fibroblasts.

In contrast to previous studies [14–16] we have shown that both SOCs and ROCs have a significant permeability for Sr^{2+}-ions. Due to the low affinity of Fura-2 for Sr^{2+}, the influx of Sr^{2+} into the cells resulted in only a rather small increase in the fluorescence ratio. This modest increase represents, however, a quite large Sr^{2+} influx. Previously we have shown that density-arrested cells can repetitively fire action potentials in calcium-free medium supplemented with strontium for prolonged periods of time [8]. Our results suggest that

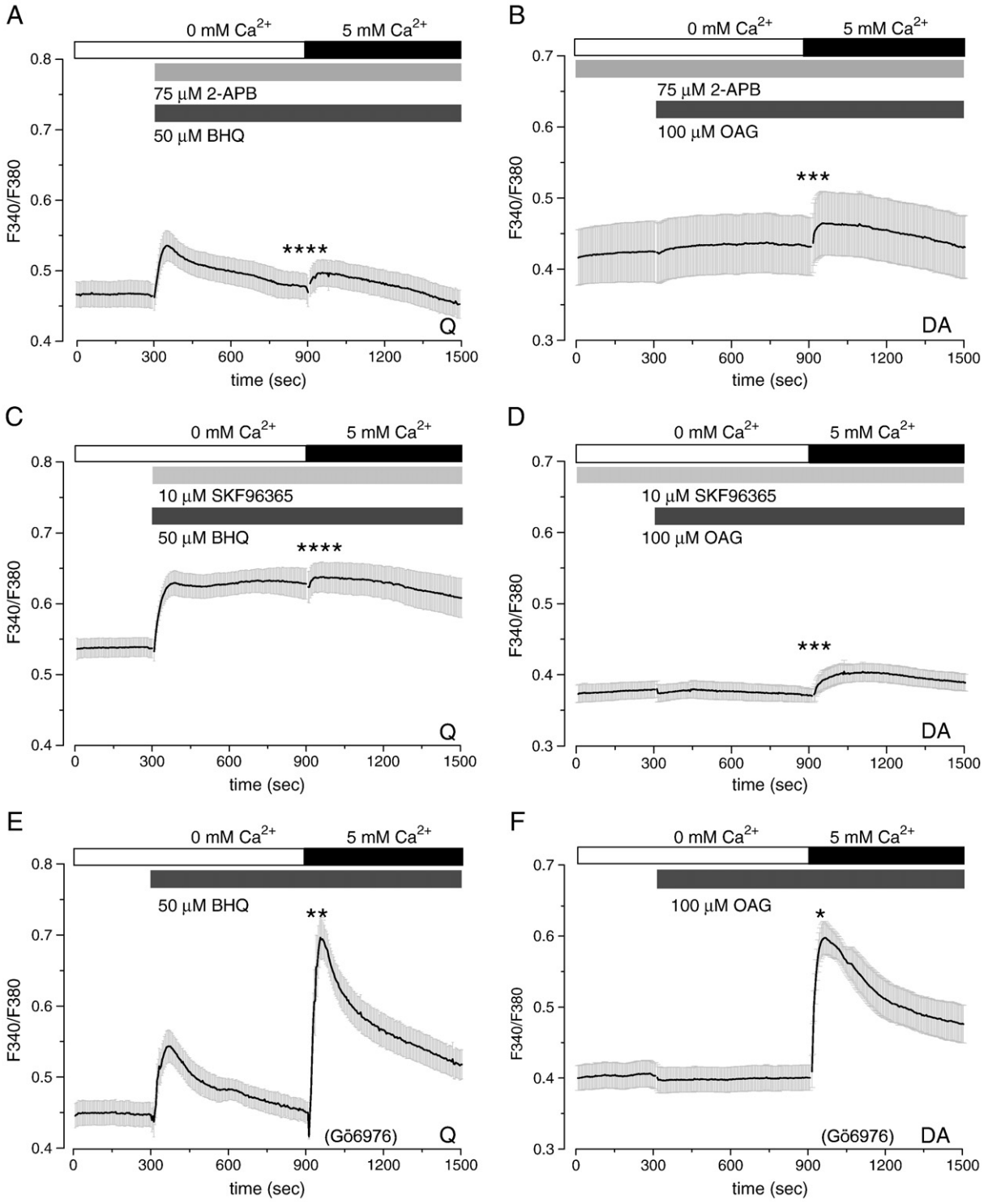

Fig. 6. Effects of pharmacological agents on calcium entry in NRK fibroblasts. A and B show the effect of 75 μM 2-APB on BHQ-induced store-operated calcium entry in quiescent cells (A) and receptor-operated calcium entry in density-arrested cells in the presence of OAG (B). C and D show the effect of SKF9365 (10 μM) on SOCE and ROCE in quiescent (C) and density-arrested cells (D), respectively. The inhibition of calcium entry by 2-APB and SKF96365 in quiescent cells is compared with control experiments (Fig. 1A) (significance: ****, $p<10^{-8}$). The inhibition of calcium entry by 2-APB and SKF96365 in density-arrested cells is compared with control experiments (Fig. 2B) (significance: ***, $p<10^{-6}$). E and F show the effect of pre-incubation (30 min) with 100 nM Gö6976 (assigned by (Gö6976) in the figure) on SOCE in quiescent (E) and ROCE in density-arrested cells (F). Potentiation of calcium entry in quiescent and density-arrested cells is compared with control experiments (Figs. 1A and **2**B, respectively) (significance: **, $p<10^{-4}$; and *, $p<0.01$). All recordings in density-arrested cells were performed in the presence of the L-type calcium channel blocker nifedipine to prevent entry of calcium through this type of calcium channels.

strontium entry is facilitated by the same activation pathways as calcium entry and that those pathways are different from the L-type voltage-gated channels.

In quiescent cells, the addition of extracellular calcium after calcium deprivation without SERCA inhibition resulted in a small calcium influx (Fig. 1C). In density-arrested cells, however, calcium addition after calcium deprivation resulted in a significantly higher calcium influx (Fig. 2C). These results indicate that density-arrested cells have another ensemble of calcium influx pathways than quiescent cells. Besides store-operated calcium entry, the density-arrested cells also exhibit a

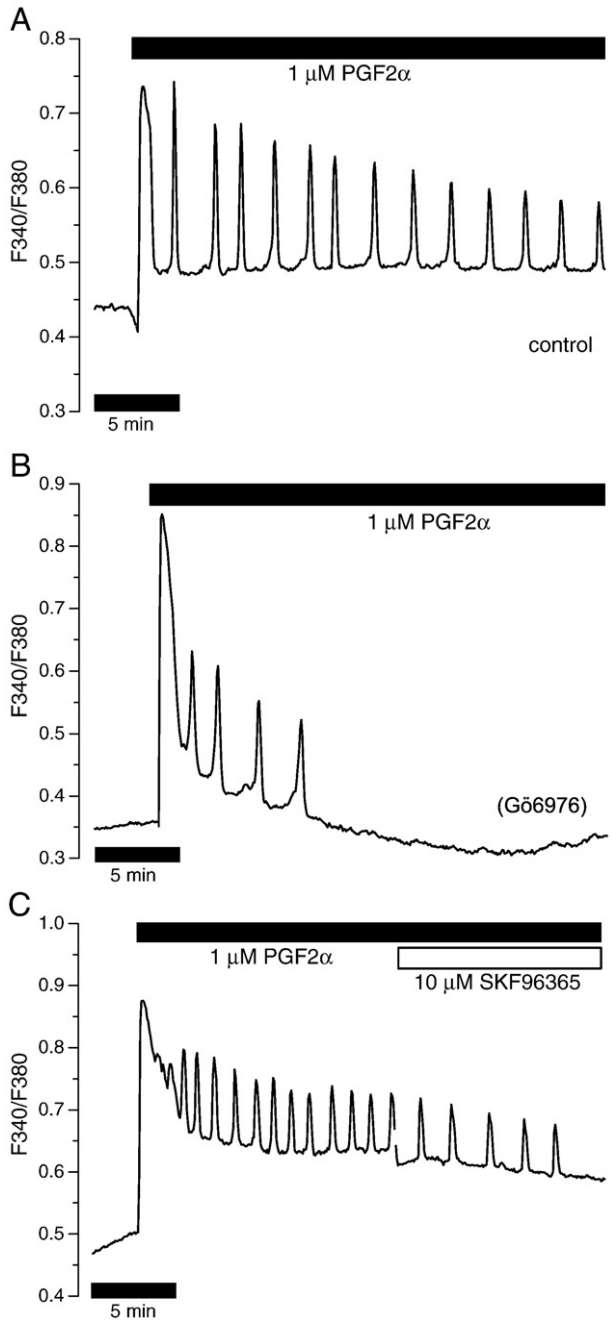

Fig. 7. SOCE modulators have a profound effect on $PGF_{2\alpha}$-induced intracellular calcium oscillations in quiescent NRK fibroblasts. (A) Intracellular calcium oscillations induced by $PGF_{2\alpha}$ in quiescent NRK fibroblasts. (B) $PGF_{2\alpha}$-induced intracellular calcium oscillations in NRK fibroblasts after 30 min pre-incubation with 100 nM Gö6976, assigned by (Gö6976) in the figure. (C) Effect of inhibition of calcium entry by 10 μM of SKF96365 on $PGF_{2\alpha}$-induced intracellular calcium oscillations in quiescent NRK fibroblasts. Each trace shown in this figure represents a typical calcium response induced by $PGF_{2\alpha}$ in an individual cell selected from a panel of 100–150 cells of data obtained in 3 independent experiments. (See Table 1 for a quantitative Mann–Whitney analysis of the significance level of the changes represented in the traces.)

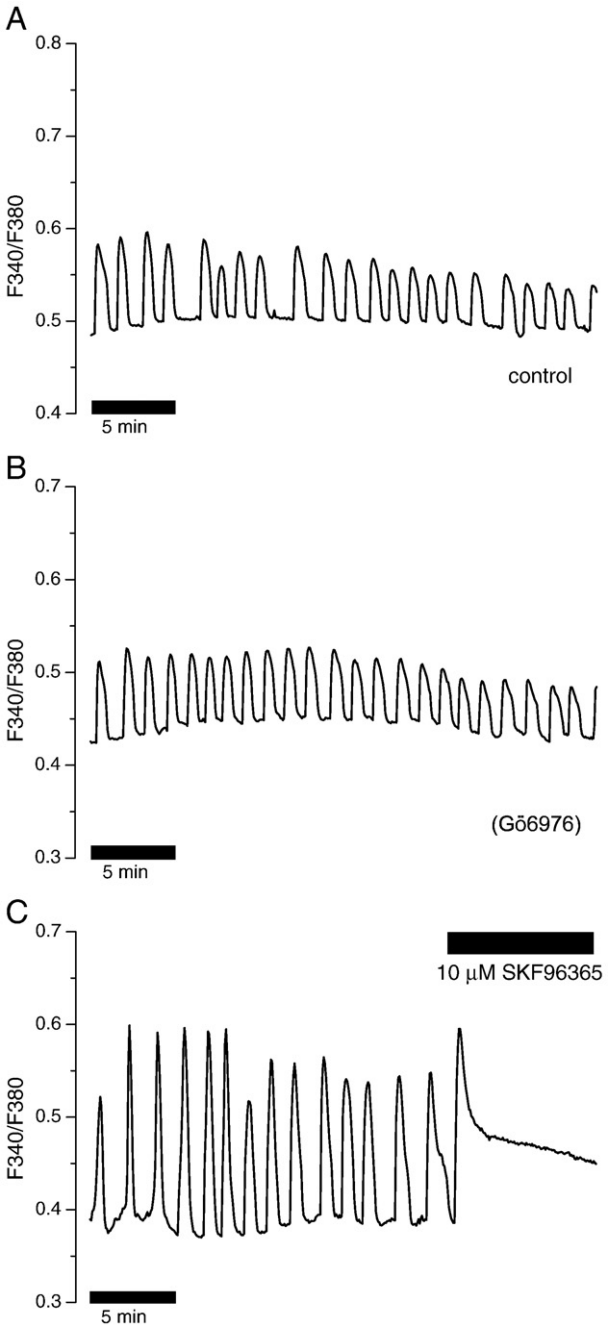

Fig. 8. Effect of either potentiating or inhibiting calcium entry on action potential-induced calcium transients in density-arrested NRK fibroblasts. (A) Calcium transients induced by propagating action potentials in density-arrested NRK fibroblasts. (B) Calcium transients induced by propagating action potentials in density-arrested NRK fibroblasts after 30 min pre-incubation with 100 nM of Gö6976, assigned by (Gö6976) in the figure. (C) Calcium transients induced by propagating action potentials in density-arrested NRK fibroblasts disappear in the presence of 10 μM SKF96365. Each trace shown in this figure represents a typical example out of 3 (pre-incubation with Gö6976) and out of 5 (addition of SKF96365) independent experiments of spontaneous synchronized calcium responses of a whole monolayer of density-arrested NRK fibroblasts, respectively. (See Table 1 for a quantitative Mann–Whitney analysis of the significance level of the changes represented in the traces.)

receptor-operated calcium entry mechanism. The addition of OAG, a DAG-derivative, did not result in an additional increase of the calcium influx. However, incubation of the density-arrested cells with PLC-inhibitor U73122 inhibited the calcium entry in these cells (Fig. 2D). This indicates that in density-arrested NRK cells a PLC-dependent hydrolysis of PIP_2 into IP_3 and DAG plays a role in the stimulation of ROCs. This is supported by earlier findings by Harks et al. [4], who have shown that density-arrested cells produce and secrete low amounts of $PGF_{2\alpha}$. This low concentration of $PGF_{2\alpha}$ activates the G-protein coupled FP receptor and activates PLC. These results suggest that the low concentrations of $PGF_{2\alpha}$ present in the culture medium of the density-arrested cells can result in an increased intracellular DAG level activating ROCE. Earlier studies [17] have proposed an $iPLA_2$-dependent pathway as an activation mechanism for SOCE. However, inhibition of $iPLA_2$ did

Table 1
Effect of Gö6976 and SKF96365 on the frequency of $PGF_{2\alpha}$-induced intracellular calcium oscillations in Q-cells and action potential-induced calcium transients in DA-cells.

Number of calcium oscillations/transients per 10 min								
	Q-cells				DA-cells			
	Median	95% Range	*n*	*p*	Median	Range	*n*	*p*
Control	7	3–16	107		7	4–8	3	
Gö6976	6	2–11	128	<0.001	6	2–7	3	>0.05
Control	6	1–10	155		6	5–9	5	
SKF96365	3	0–5	155	<0.001	1	1–3	5	<0.01

The effect of pre-incubation with Gö6976 is compared to separate control experiments. The effects of SKF96365 are compared to the $PGF_{2\alpha}$-induced calcium oscillations and the action potential-induced calcium transients, respectively, before addition of the agent. Number of calcium oscillations in a period of 10 min was counted in n individual quiescent cells from data obtained in three independent experiments. In density-arrested cells the number of synchronized calcium transients due to action potentials in the whole cellular monolayer was determined in a number (*n*) of independent experiments. The significance level (*p*) following Mann–Whitney analysis is indicated.

not affect SOCE, showing that this pathway is not relevant in NRK fibroblasts (data not shown).

Our findings are further supported by the differential expression pattern of *Trpc* genes in quiescent and density-arrested cells. Trpc channels have been described earlier as candidate channels for mediating SOCE and ROCE [18]. While the expression level of *Trpc1* was found to be independent of cell density, expression levels of *Trpc5* and *Trpc6* were clearly increased in density-arrested cells. Trpc1 is generally considered as the channel involved in SOC formation [11], while Trpc6 is known to be DAG dependent [12]. Although the exact activation pathway is not conclusive, Trpc5 seems to be activated by receptors coupled to PLC, suggesting a role together with Trpc6 in ROCE [19]. On the other hand, Zhu et al. [20] have shown that Trpc5 is desensitized by phosphorylated PKC. The binding of DAG to the C1 domain results in activation and translocation of PKC [21], whereby the production of DAG would inhibit the activity of Trpc5. The potentiating effect of PKC inhibitor Gö6976 suggests that a PKC-dependent calcium entry channel is present. However, we have shown that the PLC-inhibitor U73122, expected to decrease DAG levels, just attenuated instead of potentiated ROCE in the density-arrested NRK cells.

The six-fold increase of *Trpc6* mRNA expression coinciding with ROCE in density-arrested NRK fibroblasts suggests a prominent role of Trpc6 in ROCE. Large et al. [22] have suggested a model in which PIP_2 binds to the same binding site as DAG in the resting state of Trpc6. Cleavage of PIP_2 into IP_3 and DAG makes the DAG/PIP_2-binding site available for DAG and subsequently activates Trpc6. The requirement of both cleavage of PIP_2 and elevated DAG levels might explain the limited effect of additional OAG in combination with a significant effect of inhibiting PLC activity. Our results show a differential expression of *Trpcs*, *Orai1* and *Stim1* mRNA in quiescent and density-arrested cells coinciding with a differential regulation of ROCE and SOCE. Recently it has been reported that Stim1 converts Trpc1 from a ROC into a SOC [2,23,24] and that Trpc3, Trpc6 and Trpc7 facilitate DAG-sensitive calcium entry [12]. These studies show that an intricate interplay between Trpcs, Stim1 and Orai1 subunits may constitute the channels responsible for calcium entry, whether receptor-operated or store-operated. Our results therefore suggest that quiescent and density-arrested NRK fibroblasts differ in their calcium entry mechanisms.

The effect of SOCE inhibition and potentiation on $PGF_{2\alpha}$-induced calcium oscillations in both quiescent and spontaneously action potential firing density-arrested cells is puzzling. It was expected that an increased calcium entry in both quiescent and density-arrested cells would result in a higher frequency or amplitude of calcium oscillations and action potential-induced calcium transients, since increased calcium would fasten the recovery of the IP_3-receptor. However, in quiescent cells the calcium oscillations extinguished while density-arrested cells seemed to be unaffected by calcium entry potentiation. On the other hand, nearly complete SOCE inhibition only reduced the calcium oscillation frequency in quiescent cells by 50% (Table 1). Although inhibition of ROCE by SKF96365 in density-arrested cells was less effective than in quiescent cells (Table S3), the reduced calcium entry completely attenuated the action potential-induced calcium transients in the DA-cells (Table 1).

In NRK cells we found SOCE in quiescent cells and both SOCE and ROCE in density-arrested cells. In a previous study Kusters et al. have explored the dynamical properties of a single cell model, reproducing experimental observations on calcium oscillations and action potential generation in NRK fibroblasts [25]. An analysis of increasing SOC conductance and the effect on intracellular calcium oscillations is visualized in the bifurcation diagrams shown in Supplementary Fig. S1 (modified from [6]). This diagram shows how the range of IP_3 concentrations whereby the cells exhibit calcium oscillations, depends on store- and/or receptor-operated calcium entry. Quiescent cells start calcium oscillations after addition of $PGF_{2\alpha}$, assuming an $[IP_3]_{cyt}$ of 1 μM and a low calcium entry conductance of 0.02 nS (see Fig. S1A). Sufficient potentiation might bring these cells to an equivalent SOC level of 0.10 nS (Fig. S1C), where they become silent and depolarized. Density-arrested cells, however, behave in a more complex manner. In a previous study [26] we have suggested a pacemaker–follower system to explain the spontaneous calcium action potentials in density-arrested cells. Under conditions of density-arrest an inhomogeneity in the local production of $PGF_{2\alpha}$ might give rise to localized islands of depolarized cells with increased intracellular IP_3. In these 'pacemaker'-islands IP_3-induced intracellular calcium oscillations synchronize resulting in depolarizations at the border between polarized and depolarized cells, giving rise to propagating action potentials which depolarize the surrounding 'follower'-cells. According to Harks et al. [4] density-arrested cells have a $PGF_{2\alpha}$ concentration of only 1.5 nM in the extracellular medium. Therefore the cytosolic level of IP_3 in density-arrested cells is presumably much lower than in quiescent cells stimulated with 1 μM $PGF_{2\alpha}$. Density-arrested cells, however, seem to have a larger calcium entry facilitated by SOCs and ROCs, so in pacemaking cells the concentration of IP_3 might be in a regime near 0.2 μM in combination with a membrane calcium conductance of 0.04 nS (Fig. S1B). An increase/potentiation of calcium entry conductance (to 0.10 nS, Fig. S1C), while maintaining a constant level of $[IP_3]_{cyt}$, would not stop the calcium oscillations. This shows that the higher calcium influx in density-arrested cells results in a broader range of IP_3 concentrations that can induce calcium oscillations. Apparently, density-arrested cells are more sensitive to IP_3 with respect to the ability to induce calcium oscillations.

The effect of increasing calcium entry on the calcium oscillations in NRK cells suggests that proliferation of these cells from the quiescent to the density-arrested stage may not only result in an increased production of $PGF_{2\alpha}$, but also in an enhanced expression of both SOCs and ROCs. This differential mechanism of calcium entry provides NRK fibroblasts with an elegant pathway to meet their calcium requirements under the different growth conditions. Our previous study [6] has shown that a regulated calcium entry is required to couple membrane excitability with calcium dynamics, in order to maintain calcium homeostasis in NRK fibroblasts. Our results thereby suggest that Trpc channels, most likely in combination with Stim1 and Orai1, are able to provide this calcium entry pathway. We are currently testing this hypothesis by using a shRNA approach to selectively knockdown the genes for these proteins.

5. Conclusions

In this study we have shown that Trpc1, Trpc5 and Trpc6, Stim1 and Orai1 are expressed in NRK fibroblasts. Moreover, Trpc5, Trpc6 and Orai1 are differentially expressed in quiescent and density-arrested cells. The increased expression of these genes in density-arrested cells coincides with an increase of SOCE and ROCE at this growth stage. The involvement of Trpc6 in ROCE is supported by our observation that

ROCE is a PLC-dependent process. Earlier observations of sustained oscillations in Sr^{2+}-containing media are supported by our finding that in NRK fibroblasts SOCs as well as ROCs are not only permeable for Ca^{2+} but also for Sr^{2+}. The earlier notion from the mathematical model of NRK fibroblasts that calcium entry limits the range in which IP_3-dependent calcium oscillations and action potentials can occur, is supported by the present experimental findings.

Acknowledgements

We gratefully thank professor D.L. Ypey (Department of Cell Biology, Radboud University Nijmegen) for his interest and valuable advices during the course of this study. This research project was funded by the Physical Biology Research Program (no. 805.47.066) of the Stichting voor Fundamenteel Onderzoek der Materie (FOM) and the Gebiedsbestuur Aard en Levenswetenschappen (ALW), which are financially supported by the Netherlands Organization for Scientific Research (NWO).

Appendix A. Supplementary data

Supplementary data associated with this article can be found, in the online version, at doi:10.1016/j.cellsig.2010.02.007.

References

[1] J.W. Putney, Immunol. Rev. 231 (1) (2009) 10.
[2] M.D. Cahalan, Nat. Cell Biol. 11 (6) (2009) 669.
[3] G.M. Salido, S.O. Sage, Rosado JA, Biochim. Biophys. Acta 1793 (2) (2009) 223.
[4] E.G. Harks, P.H. Peters, J.L. van Dongen, E.J. van Zoelen, A.P. Theuvenet, Am. J. Physiol. Cell. Physiol. 289 (1) (2005) C130.
[5] E.G. Harks, W.J. Scheenen, P.H. Peters, E.J. van Zoelen, A.P. Theuvenet, Pflugers Arch. 447 (1) (2003) 78.
[6] J.M. Kusters, M.M. Dernison, v.W.P. Meerwijk, D.L. Ypey, A.P. Theuvenet, C.C. Gielen, Biophys. J. 89 (6) (2005) 3741.
[7] L.N. Cornelisse, R. Deumens, J.J. Coenen, E.W. Roubos, C.C. Gielen, D.L. Ypey, B.G. Jenks, W.J. Scheenen, J. Neuroendocrinol. 14 (10) (2002) 778.
[8] A.D. de Roos, P.H. Willems, P.H. Peters, E.J. van Zoelen, A.P. Theuvenet, Cell Calcium 22 (3) (1997) 195.
[9] J. Hatae, N. Fujishiro, H. Kawata, Jpn. J. Physiol. 46 (5) (1996) 423.
[10] J.A. Robinson, N.S. Jenkins, N.A. Holman, S.J. Roberts-Thomson, G.R. Monteith, J. Biochem. Biophys. Methods 58 (3) (2004) 227.
[11] X. Liu, B.B. Singh, I.S. Ambudkar, J. Biol. Chem. 278 (13) (2003) 11337.
[12] L. Lemonnier, M. Trebak, J.W. Putney Jr., Cell Calcium 43 (5) (2008) 506.
[13] A. Siefjediers, M. Hardt, G. Prinz, M. Diener, Cell Calcium 41 (4) (2007) 303.
[14] A. Gamberucci, E. Giurisato, P. Pizzo, M. Tassi, R. Giunti, D.P. McIntosh, A. Benedetti, Biochem. J. 364 (Pt 1) (2002) 245.
[15] K. Venkatachalam, F. Zheng, D.L. Gill, J. Biol. Chem. 278 (31) (2003) 29031.
[16] Y. Tesfai, H.M. Brereton, G.J. Barritt, Biochem. J. 358 (pt 3) (2001) 717.
[17] M. Flourakis, F. Van Coppenolle, V. Lehen'kyi, B. Beck, R. Skryma, N. Prevarskaya, FASEB J. 20 (8) (2006) 1215.
[18] A.B. Parekh, J.W. Putney Jr., Physiol. Rev. 85 (2) (2005) 757.
[19] N.T. Blair, J.S. Kaczmarek, D.E. Clapham, J. Gen. Physiol. 133 (5) (2009) 525.
[20] M.H. Zhu, M. Chae, H.J. Kim, Y.M. Lee, M.J. Kim, N.G. Jin, D.K. Yang, I. So, K.W. Kim, Am. J. Physiol. Cell. Physiol. 289 (3) (2005) C591.
[21] A.C. Newton, Chem. Rev. 101 (8) (2001) 2353.
[22] W.A. Large, S.N. Saleh, A.P. Albert, Cell Calcium (2009).
[23] S. Alicia, Z. Angelica, S. Carlos, S. Alfonso, L. Vaca, Cell Calcium 44 (5) (2008) 479.
[24] I. Jardin, J.J. Lopez, G.M. Salido, J.A. Rosado, J. Biol. Chem. 283 (37) (2008) 25296.
[25] J.M. Kusters, J.M. Cortes, W.P. van Meerwijk, D.L. Ypey, A.P. Theuvenet, C.C. Gielen, Phys. Rev. Lett. 98 (9) (2007) 098107.
[26] M.M. Dernison, J.M. Kusters, P.H. Peters, W.P. van Meerwijk, D.L. Ypey, C.C. Gielen, E.J. van Zoelen, A.P. Theuvenet, Cell Calcium 44 (5) (2008) 429.